Supported oxides catalysts for the dehydration of isobutanol into butenes: relationships between acidic and catalytic properties

Z. Buniazet[1,2] A. Cabiac,[2] S. Maury,[2] S. Loridant[1,*]

[1] *Institut de Recherches sur la Catalyse et l'Environnement de Lyon, IRCELYON, CNRS-Université Claude Bernard Lyon 1, 2 av. Einstein, F-69626 Villeurbanne Cedex, France*

[2] *IFP Energies nouvelles, Rond-point de l'échangeur de Solaize, BP 3, F-69360 Solaize, France*

* Corresponding Author: Ph. + 33 [0] 472 445 334, Fax + 33 [0] 472 445 399, E-mail stephane.loridant@ircelyon.univ-lyon1.fr

Table S1. XPS Binding Energies of the Si 2p, Sn $3d_{5/2}$, Ti $2p_{3/2}$ and O 1s bands observed for different compounds.

	Binding Energy (eV)					ICP
Catalyst	Si 2p	Sn $3d_{5/2}$	Ti $2p_{3/2}$	O 1s	M/Si	M/Si
26.0% SnO_2/SiO_2-G	103.3	487.3	-	532.6 (79%) 530.8 (21%)	0.49	0.14
20.4%TiO_2/SiO_2-G	103.3	-	459.0	532.6 (92%) 530.8 (8%)	0.15	0.19
TiO_2-P25	-	-	458.5	529.7	-	-
SiO_2	103.5	-	-	532.6	-	-

Table S2. Shift of the ν(C≡O) band of CO molecules coordinated to Lewis sites compared to physisorbed CO molecules (2136 cm^{-1}) and shift of the ν(O-H) bands located at 3720-3740 cm^{-1}.

Compound	Shift of the ν(C≡O) band (cm^{-1})	Shift of the ν(O-H) bands (cm^{-1})
26.0% SnO_2/SiO_2-G	+51	-100
20.4% TiO_2/SiO_2-G	+51 ; +42	-102
15.9% WO_3/SiO_2-G	+77 ; +45 ; +33	-90
39.7% WO_3/SiO_2-G	+72 ; +44	-
18.5% $H_4SiW_{12}O_{40}/SiO_2$-G	+45	-100

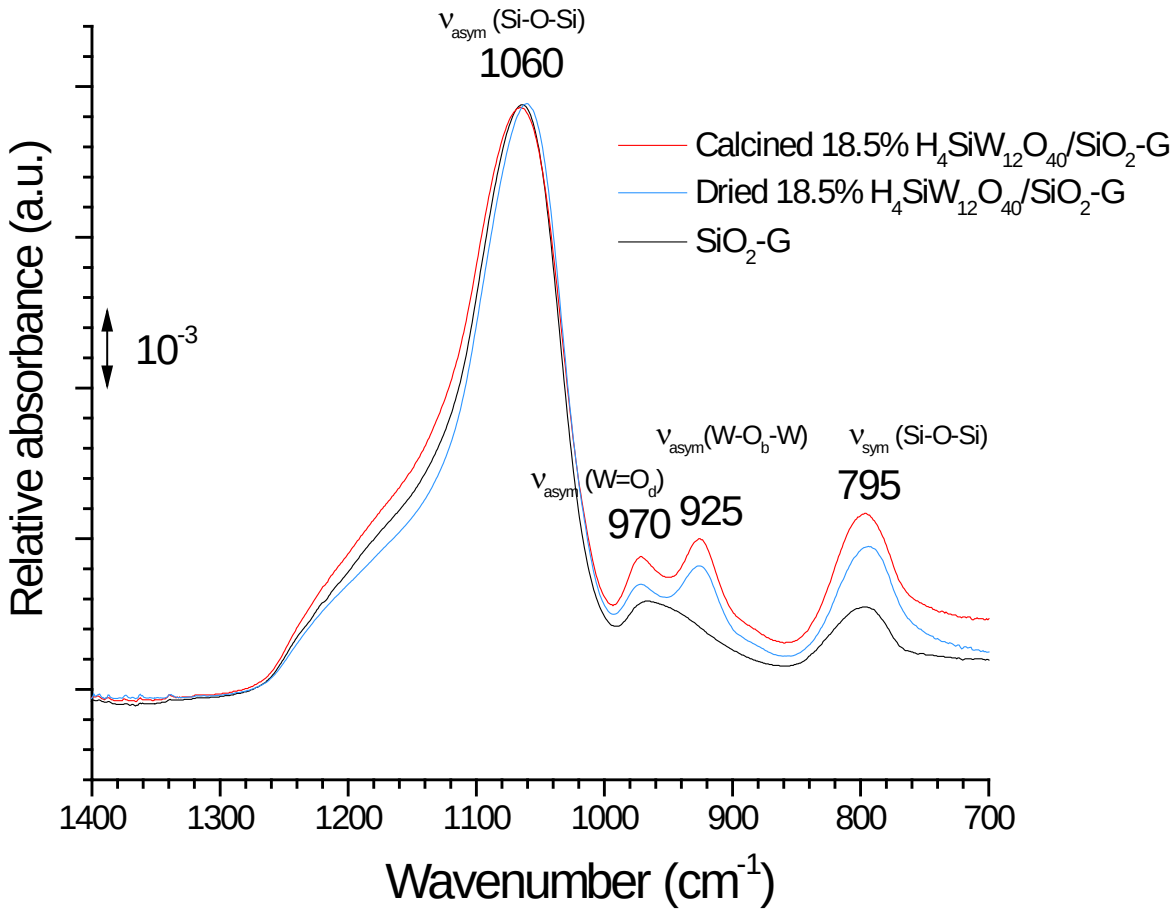

Figure S1. ATR IR spectra of the SiO_2-G support, dried and calcined 18.5%$H_4SiW_{12}O_{40}/SiO_2$-G solids. The vibrational bands of SiO_2 and $H_4SiW_{12}O_{40}$ were attributed from [42-44].

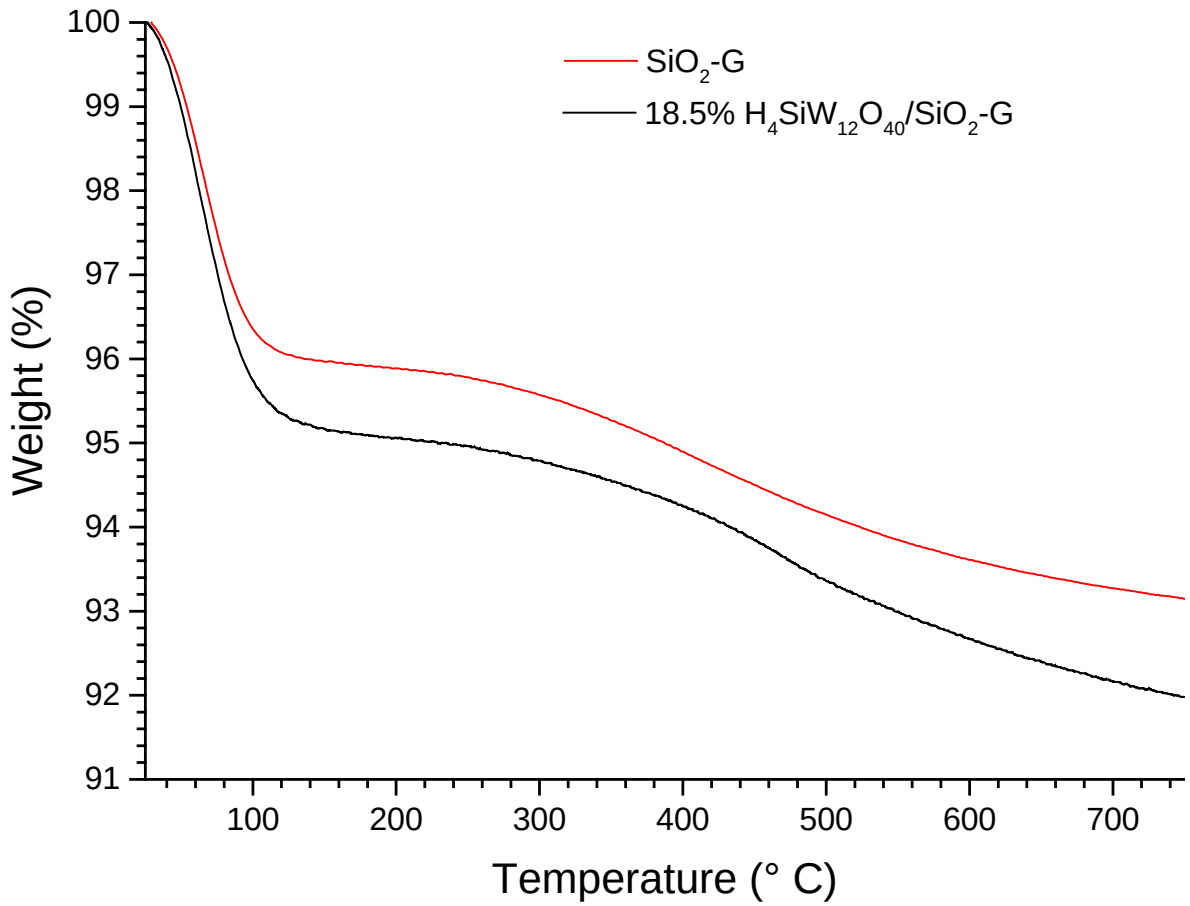

Figure S2. TGA curves of the SiO_2-G support and 18.5%$H_4SiW_{12}O_{40}/SiO_2$-G compound.

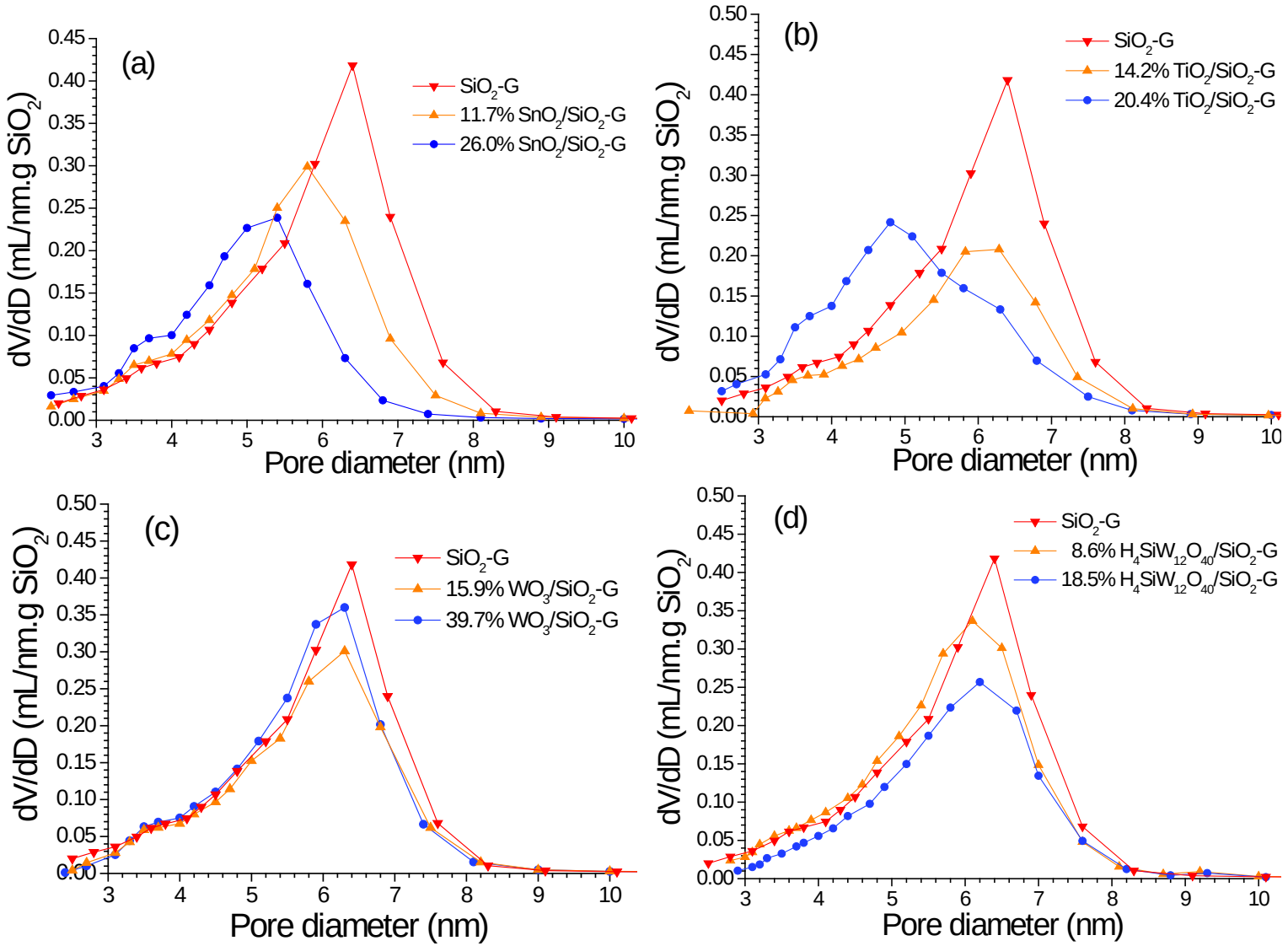

Figure S3. Pore diameter distributions of (a) SnO_2/SiO_2-G, (b) TiO_2/SiO_2-G, (c) WO_3/SiO_2-G and (d) $H_4SiW_{12}O_{40}/SiO_2$-G compounds.

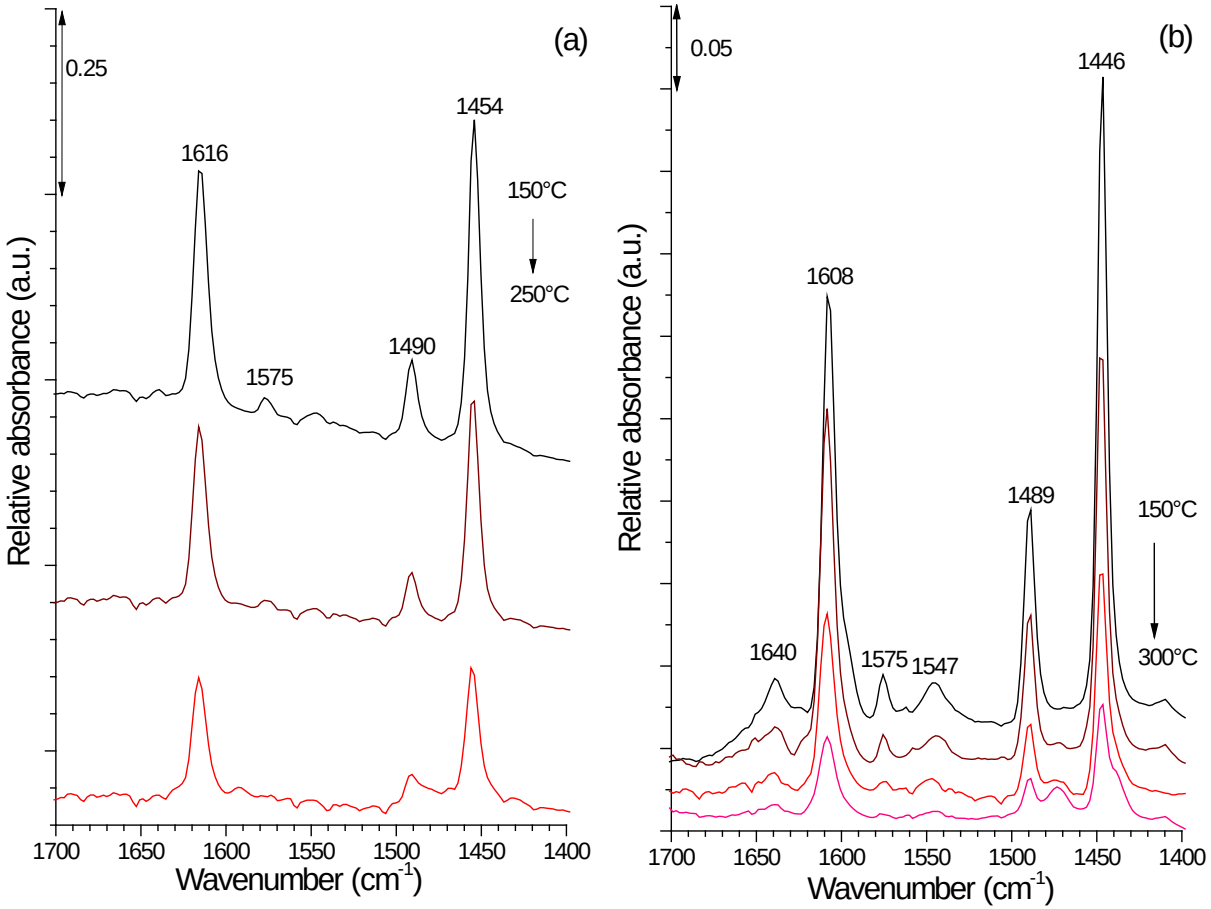

Figure S4. (a) Evolution of the IR spectrum of pretreated (a) 26.0%TiO_2/SiO_2-G, (b) 20.4%TiO_2/SiO_2-G compounds recorded upon adsorption of pyridine at RT and followed by evacuation at increasing temperatures. The background corresponded to the spectrum recorded at RT under dry air flow after pretreatment.

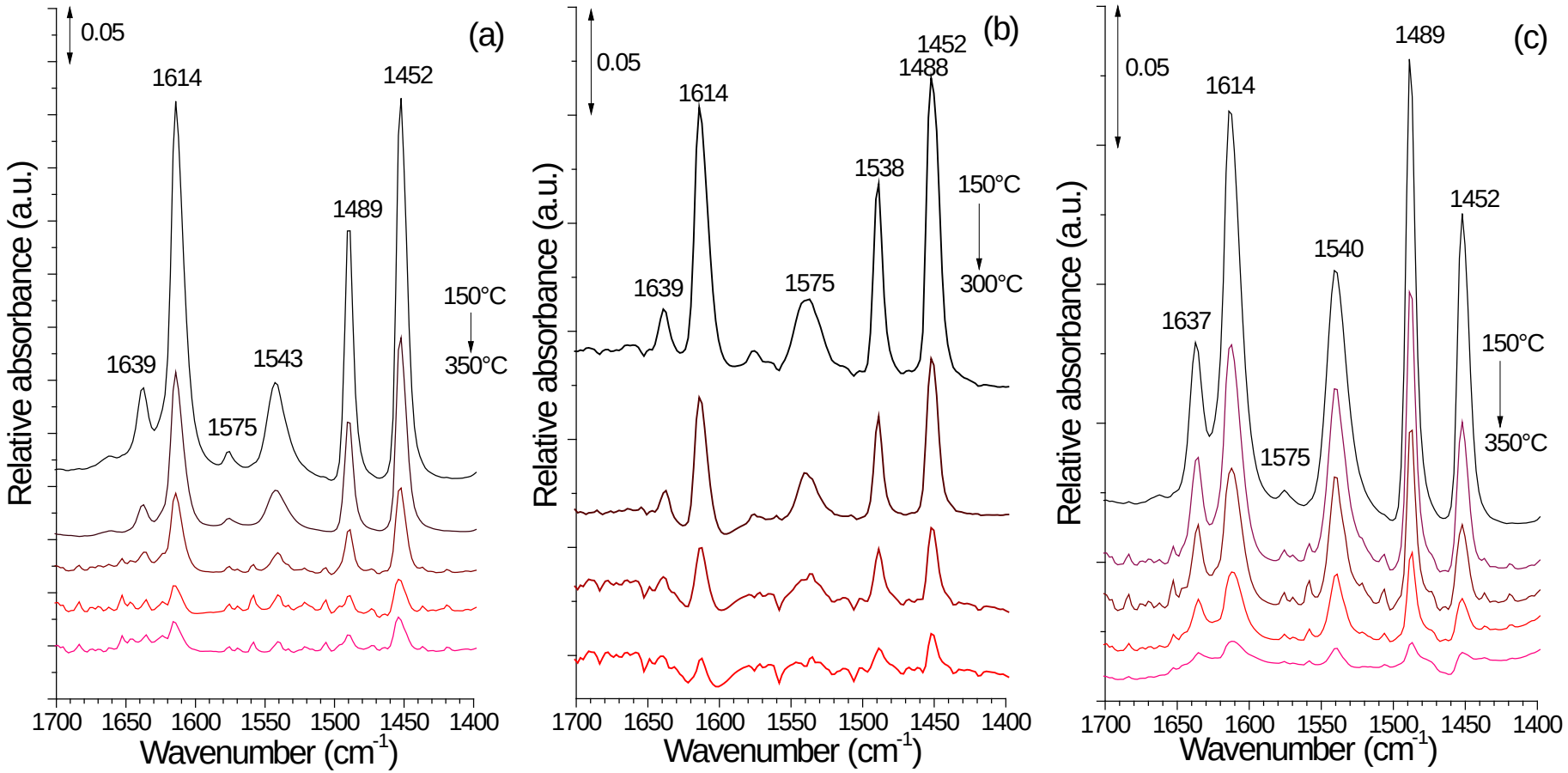

Figure S5. (a) Evolution of the IR spectrum of pretreated (a) 15.9%WO_3/SiO_2-G, (b) 39.7%WO_3/SiO_2-G and (c) 18.5%$H_4SiW_{12}O_{40}/SiO_2$-G compounds recorded upon adsorption of pyridine at RT and followed by evacuation at increasing temperatures. The background corresponded to the spectrum recorded at RT under dry air flow after pretreatment.

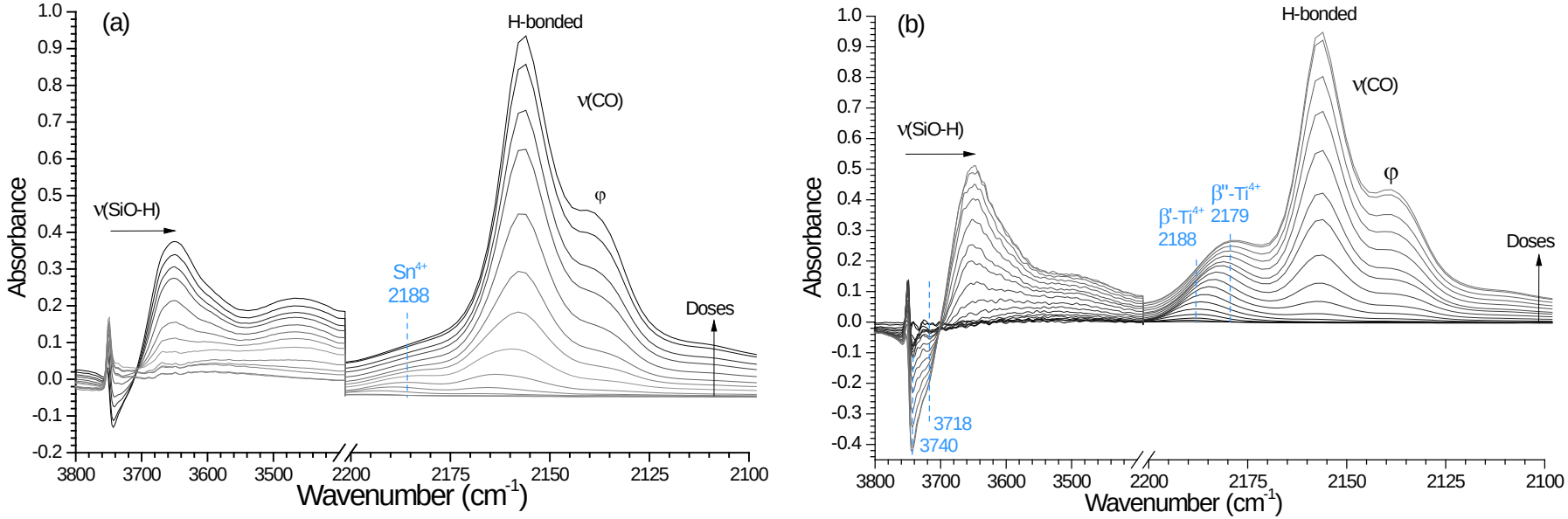

Figure S6. Evolution of the IR spectrum of pretreated (a) 26.0%SnO_2/SiO_2-G, (b) 20.4%TiO_2/SiO_2-G compounds upon adsorption of increasing doses of CO at 77 K. The background corresponded to the spectrum recorded at 77 K after pretreatment.

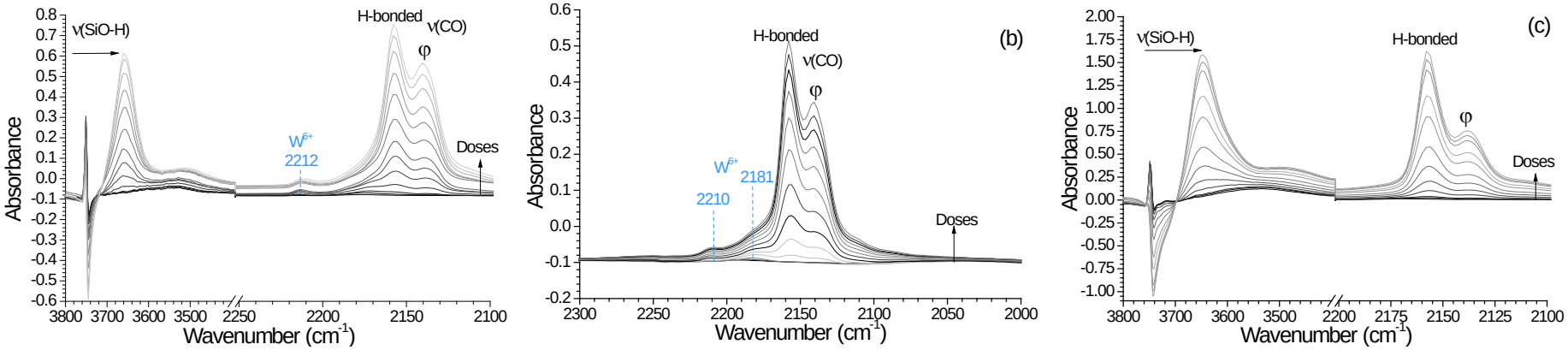

Figure S7. Evolution of the IR spectrum of pretreated (a) 15.9%WO_3/SiO_2-G, (b) 39.7%WO_3/SiO_2-G and (c) 18.5%$H_4SiW_{12}O_{40}/SiO_2$-G compounds upon adsorption of increasing doses of CO at 77 K. The background corresponded to the spectrum recorded at 77 K after pretreatment.

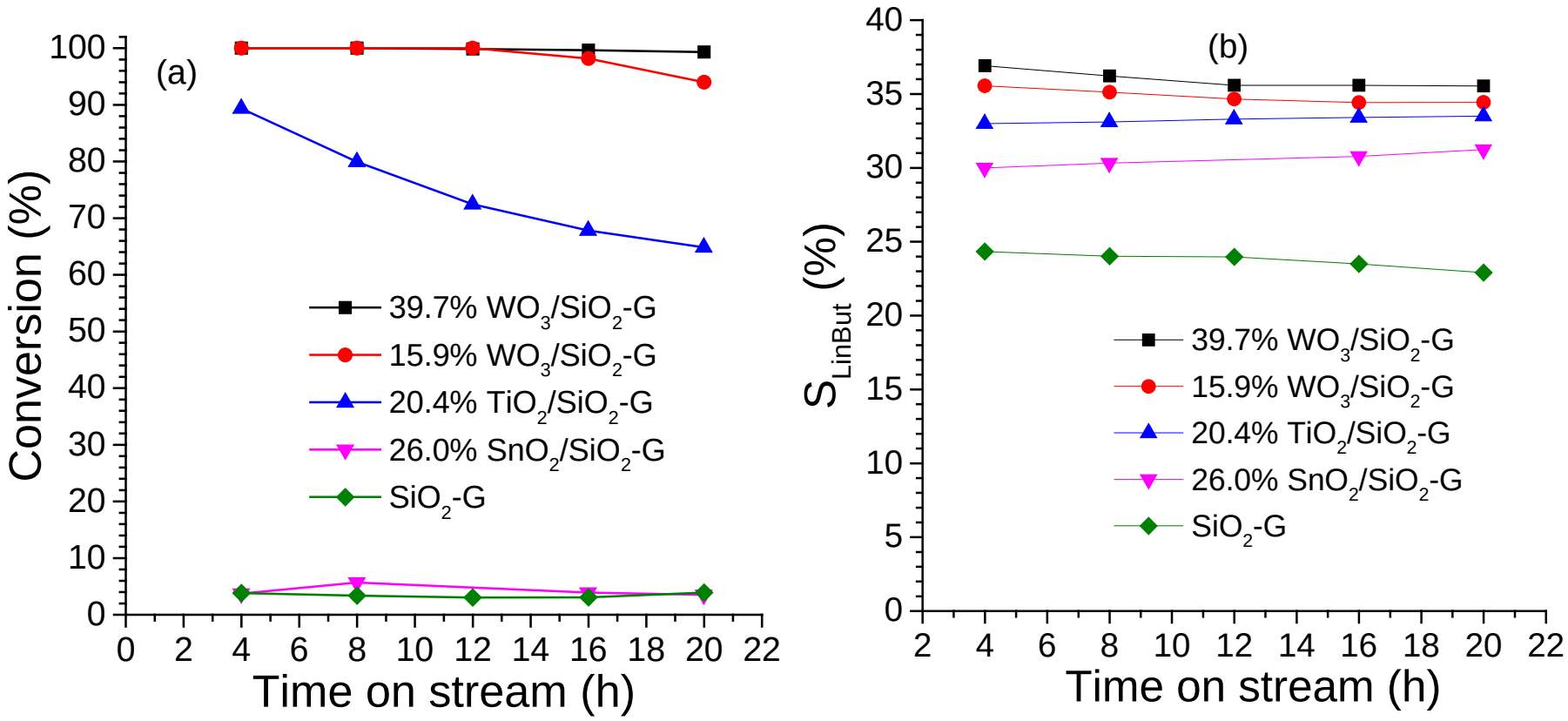

Figure S8. Evolutions of (a) the conversion and (b) the S_{LinBut} value with the time on stream for the different screened catalysts.

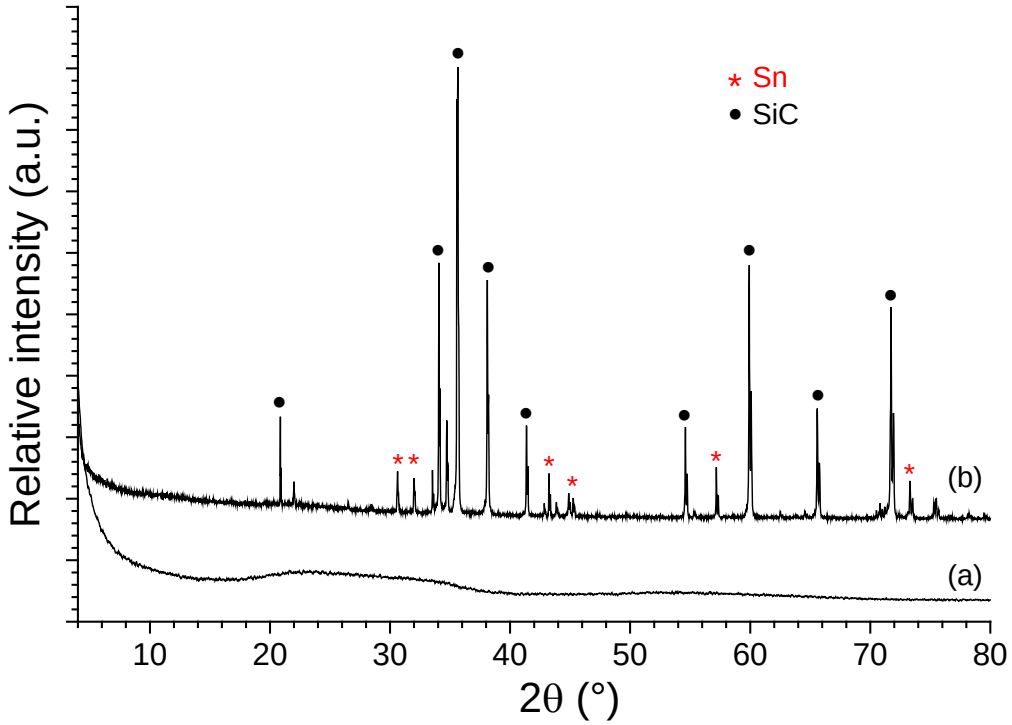

Figure S9: XRD pattern of 26.0%SnO_2/SiO_2-G (a) before and (b) after 20 h of catalytic testing at 300 °C, 1/WHSV 0.33 h. *: Sn tetragonal structure (ICDD: 01-089-2761), ●: SiC hexagonal structure (ICDD: 04-012-5685).

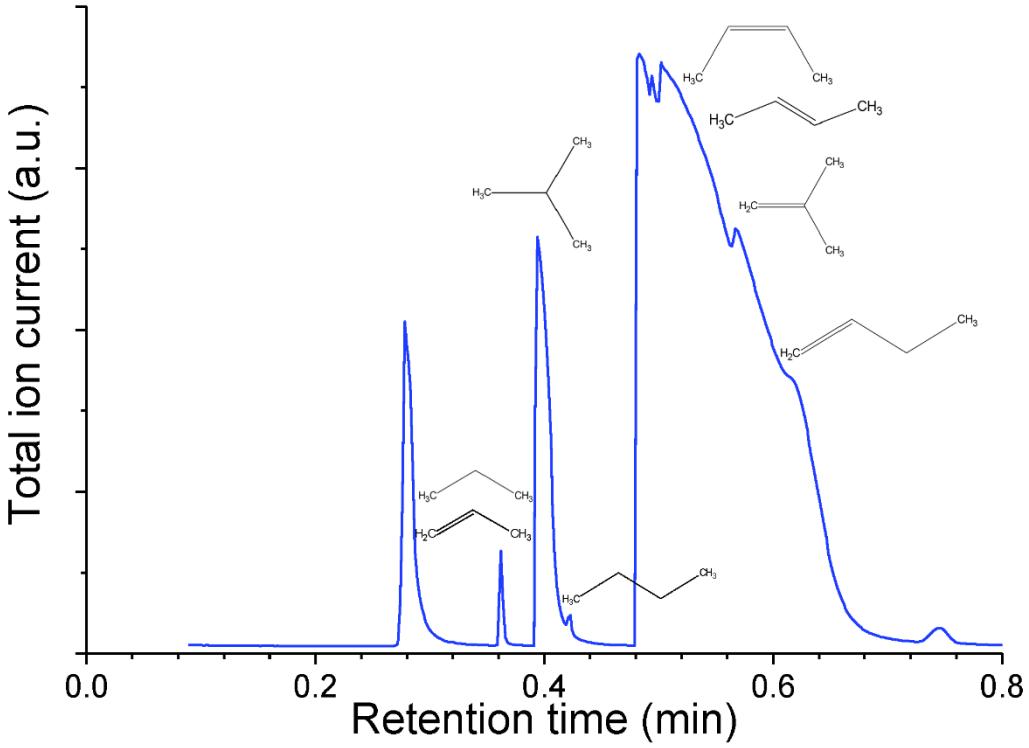

Figure S10. μGC-MS analysis of gas phase during catalytic testing of 18.5% $H_4SiW_{12}O_{40}/SiO_2$-G. Feed composition iC_4OH/inert = 30/70, temperature 175 °C, 1/WHSV 0.37 h, time 24 h.

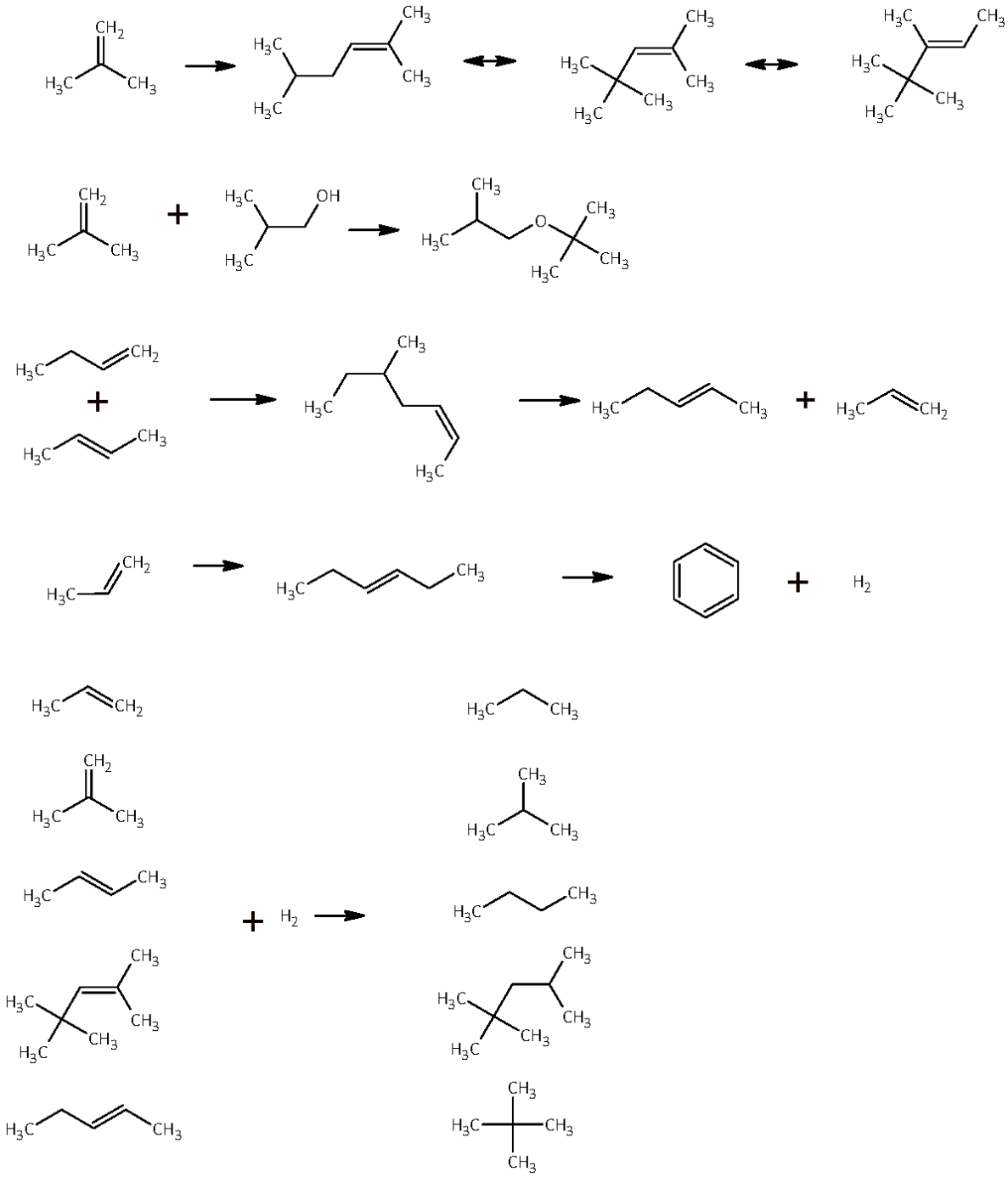

Figure S11. Formation and consecutive reaction of secondary products.

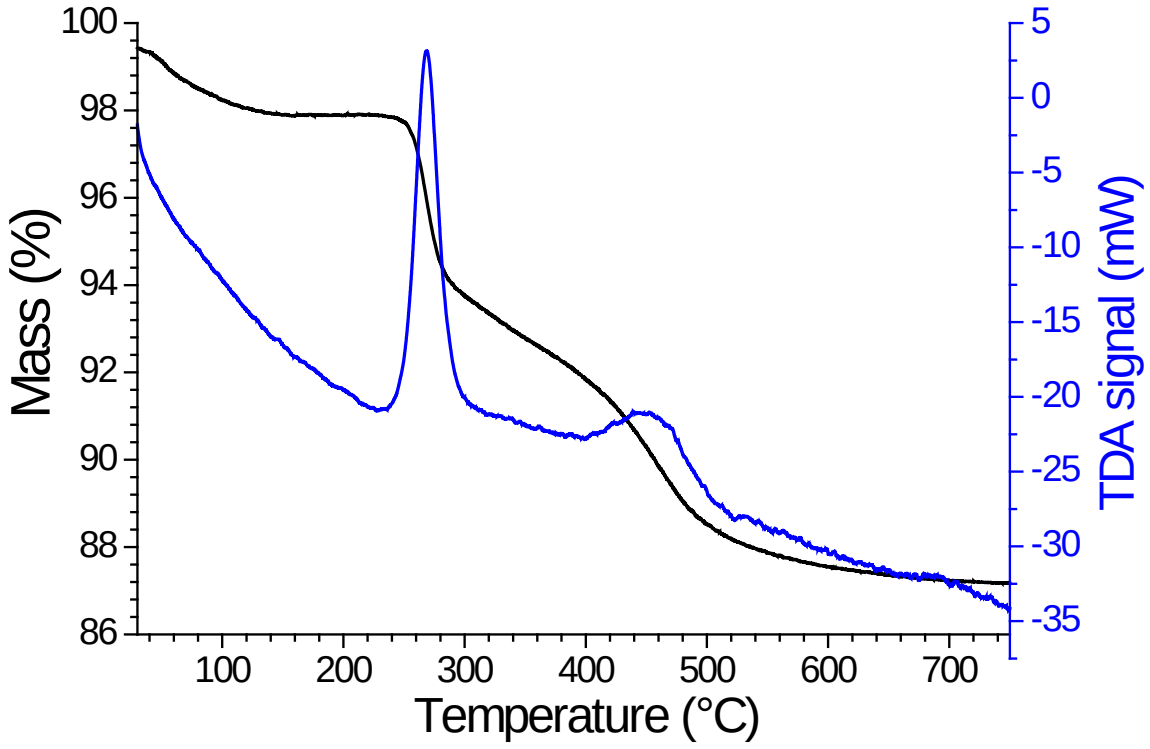

Figure S12. TGA and TDA curves obtained with 18.5% $H_4SiW_{12}O_{40}/SiO_2$-G compound after catalytic testing. Feed composition iC_4OH/inert = 30/70, temperature 175 °C, 1/WHSV 0.37 h, time 24 h.